



International Journal of Information and Communication Technology

ISSN online: 1741-8070 - ISSN print: 1466-6642

<https://www.inderscience.com/ijict>

3D point clouds recognition method for substation equipment using a new attribute descriptor method

Gang Yang, Na Zhang, Shucai Li, Fan Hu, Jichong Liang, Dawei Wang

DOI: [10.1504/IJICT.2025.10071592](https://doi.org/10.1504/IJICT.2025.10071592)

Article History:

Received:	20 December 2024
Last revised:	05 March 2025
Accepted:	05 March 2025
Published online:	20 June 2025

3D point clouds recognition method for substation equipment using a new attribute descriptor method

Gang Yang and Na Zhang*

State Grid Shanxi Electric Power Research Institute,
Taiyuan, Shanxi, 030001, China
Email: yanggang9800@163.com
Email: xiedongnan@ldy.edu.rs
*Corresponding author

Shuca Li

State Grid Shanxi Lvliang Power Supply Company,
Lvliang, Shanxi, 033000, China
Email: louyimei@ldy.edu.rs

Fan Hu, Jichong Liang and Dawei Wang

State Grid Shanxi Electric Power Research Institute,
Taiyuan, Shanxi, 030001, China
Email: hitszhufan@163.com
Email: liangjichong@sx.sgcc.com.cn
Email: davidsgcc@126.com

Abstract: As smart grids evolve, substation point cloud data is vital for management, maintenance, and monitoring. However, traditional recognition algorithms struggle with challenges such as noise, occlusion, viewpoint changes, and uneven density. This paper proposes a novel approach for substation equipment point cloud recognition. It first establishes a local coordinate system for the point cloud based on symmetry and spatial distribution, achieving translation and rotation invariance. A new attribute descriptor is then defined, considering form characteristics and viewpoint variations, and a template database of 20 electrical devices is created. By matching descriptor of a device's point cloud with those in the template database, the correct device is identified. The proposed method is compared with two other methods, achieving a 90% identification precision with an average time of 3.2 seconds per device. The method demonstrates robustness, maintaining over 70% accuracy even with noise, occlusion, and irregular point cloud density.

Keywords: substation equipment; point cloud recognition; local coordinate system; attribute descriptor; matching descriptor.

Reference to this paper should be made as follows: Yang, G., Zhang, N., Li, S., Hu, F., Liang, J. and Wang, D. (2025) '3D point clouds recognition method for substation equipment using a new attribute descriptor method', *Int. J. Information and Communication Technology*, Vol. 26, No. 21, pp.1–22.

Biographical notes: Gang Yang is a Senior Engineer. He is working at State Grid Shanxi Electric Power Research Institute. His research interests include intelligent diagnosis technology for power equipment status.

Na Zhang is a Senior Engineer. She is working at State Grid Shanxi Electric Power Research Institute. Her research interests include visual intelligent diagnosis technology for power equipment.

Shucui Li is an Engineer. He is working at State Grid Shanxi Lvliang Power Supply Company. His research interests include power equipment testing technology.

Fan Hu is a Senior Engineer. He is working at State Grid Shanxi Electric Power Research Institute. His research interests include intelligent recognition technology for power image.

Jichong Liang is a Senior Engineer. He is working at State Grid Shanxi Electric Power Research Institute. His research interests include state evaluation technology for substation equipment.

Dawei Wang is an Engineer. He is working at State Grid Shanxi Electric Power Research Institute. His research interests include electric power visual security prevention and control technology.

1 Introduction

In recent years, 3D reconstruction technology has been widely used in computer vision, robot navigation, intelligent monitoring, and other fields (Sun et al., 2021). Especially in infrastructure management and maintenance, high-precision 3D modelling can provide more intuitive and accurate environmental information, which can help intelligent operation and maintenance, and fault detection. As a core component of the power system, substations have a wide variety of equipment and complex structures. Traditional inspection and management methods often rely on manual operation, which is inefficient and easily affected by human factors. Therefore, how to use advanced 3D reconstruction technology to realise intelligent management of substations has become an important direction of current research (Karantzalos and Paragios, 2010; Zhu et al., 2024).

Traditional substation 3D modelling methods mainly rely on engineering blueprints and professional 3D modelling software (such as 3DMax) (Azevedo et al., 2021; Kokorus et al., 2016). However, this approach faces many challenges: first, the construction process of the substation may cause the final structure to be inconsistent with the original design drawings due to factors such as construction changes and equipment replacement; second, the engineering drawings may be outdated and incomplete, making it difficult for the blueprint-based modelling method to guarantee high accuracy; in addition, the manual comparison and manual modelling processes are cumbersome and error-prone, affecting the efficiency and quality of modelling (Wu et al., 2018; Zhang et al., 2023).

Driven by advancements in laser scanning and building information modelling (BIM) technologies, Zhang et al. (2024) and Ye et al. (2023) have highlighted that 3D reconstruction utilising point cloud data has gradually become an effective solution.

By using laser scanning and BIM technologies, more accurate 3D structural information of substations can be captured, and discrepancies between design and actual construction can be detected promptly. Studies have shown that this approach notably enhances the precision and effectiveness of 3D modelling, particularly when handling incomplete construction data and outdated design data (Ye et al., 2023; Hu, 2020). Additionally, Ye et al. (2023) believe that the application of 3D modelling software (such as 3DMax) is continuously optimised. By combining point cloud data with engineering drawings, manual comparison errors in traditional methods can be effectively resolved.

Currently, for 3D recognition of substation equipment, features such as projected boundary curvature and point cloud intensity are used, along with an improved AdaBoost algorithm for equipment recognition, achieving over 98% accuracy in both training and testing. However, the computation time is relatively long (Jawad et al., 2020; Yuan et al., 2022). While AdaBoost performs excellently in classification accuracy, the use of numerous weak classifiers leads to longer computation times, limiting its real-time efficiency in practical substation applications. Therefore, further optimisation to balance recognition accuracy and computation time remains a key research direction.

To obtain a depth image of the point cloud, preselection results are obtained by calculating the histogram similarity of distances to model libraries, and the most matching model is selected through Hough voting, achieving a recognition rate of 90.1% with an average recognition time of 15.6 seconds (Li et al., 2023b; Yang et al., 2024). This method improves matching efficiency and recognition rate by using histogram similarity as a point cloud preprocessing step. Hough voting effectively reduces misrecognition and enhances stability. Furthermore, this method outperforms the AdaBoost algorithm in terms of computation time, making it more suitable for real-time recognition in substation equipment scenarios. However, in cases with more complex point cloud data or numerous equipment types, issues with inaccurate similarity measurement may arise, requiring further research and optimisation.

The device point cloud base completes partial identification and segmentation, but does not complete device identification (Yuan et al., 2022). Their method focuses on extracting sub-base point clouds of substation equipment through segmentation algorithms, laying the foundation for subsequent equipment recognition and scene reconstruction. However, since this method does not complete full equipment recognition, it cannot be directly applied for comprehensive substation equipment detection and monitoring. To overcome this limitation, future research could combine advanced techniques such as deep learning to further recognise and classify equipment, improving accuracy.

Some scholars first divide the bounding box of substation equipment point clouds into subspaces. Nader et al. (2021) optimised the feature weights of subspaces using particle swarm optimisation (PSO) and then used the K-nearest neighbour (KNN) algorithm for classification (Yang et al., 2024). By dividing point cloud data into multiple subspaces, the method effectively reduces computational complexity and uses PSO to optimise feature weights, thereby improving classification accuracy. However, this method is sensitive to noise, especially when point cloud data is of poor quality or contains significant background noise, which can affect recognition results. To address this, recent studies have attempted to integrate deep learning models to enhance noise robustness, but the issue of high algorithm complexity remains.

Sun et al. (2022) first extract geometric features from the coloured point cloud, then determine the optimal feature subset, and finally use the random forest algorithm to classify the point cloud. Al-Durgham (2014) used the RANSAC algorithm to extract semi-surface features for model preselection, followed by key point extraction based on point cloud curvature information, and precise recognition through the iterative closest point (ICP) algorithm. This method reduces computational load by initially extracting features using RANSAC and achieves precise matching through ICP. Although this method excels in recognition accuracy, the computation time is long, particularly in large-scale substation equipment point cloud data processing, where ICP requires numerous iterations, resulting in poor real-time performance. Thus, optimising computation time while ensuring accuracy remains a significant research challenge.

Numerous studies (Arastounia and Lichti, 2015; Arastounia and Lichti, 2013; Arastounia and Lichti, 2014; Zhang et al., 2018) in leverage prior knowledge of equipment models to automatically extract specific equipment models, such as insulators, transformers and circuit breakers (Yu et al., 2021). These studies combine prior knowledge with point cloud data to improve equipment recognition efficiency and reduce interference from irrelevant objects. However, reliance on prior knowledge limits the generalisation ability of these methods, particularly when faced with new, unseen equipment models.

Zhang et al. (2024) divided the bounding box and used the point count within each segment as features for equipment 3D data recognition, achieving fast recognition speed, but without considering the posture of the equipment 3D data. This method is advantageous in terms of fast calculation and high recognition efficiency, making it suitable for real-time detection tasks. However, it does not effectively account for posture changes (such as rotation and translation), which may reduce recognition accuracy when dealing with equipment point clouds in different postures. Therefore, future research can enhance this method by introducing posture-invariant features or employing posture estimation techniques to improve applicability and accuracy.

This study introduces an innovative substation equipment 3D data identification method aimed at overcoming the limitations of traditional 3D data recognition methods in handling uneven density, posture variations, and noise interference. This method not only enables efficient and rapid equipment point cloud recognition but also demonstrates significant improvements in recognition accuracy. First, a local coordinate system for the equipment point cloud is constructed, effectively avoiding the impact of posture changes (such as rotation or scaling) on recognition results, while reducing errors during point cloud data transformation.

Next, to better describe the spatial form of the equipment characteristics, the paper combines the shape characteristics from the 3D data with differences at various viewing angles, designing a feature descriptor. This descriptor captures local spatial data regarding the equipment 3D model and remains stable across different viewpoints. This method enhances the feature representation capability from the 3D data and ensures elevated recognition accuracy even with uneven 3D data density. This innovation not only strengthens the 3D model's descriptive power but also reduces errors caused by viewpoint changes, thus improving robustness.

In terms of recognition efficiency, the proposed method significantly enhances recognition speed. Experimental results show that the average recognition time for each equipment is only 3.2 seconds, which adequately satisfies real-time criteria of large-scale substations. Compared with traditional equipment 3D model recognition algorithms, this

approach demonstrates notable advantage during recognition performance, making it especially suitable for environments with an array of equipment as well as large 3D model data volumes. This method ensures both efficient processing speed and elevated recognition accuracy, making substation real-time monitoring and maintenance more efficient.

The key findings of this study are outlined as follows:

- A localised coordinate system construction method for equipment 3D data is proposed, effectively avoiding the impact of posture variations (such as rotation or scaling) and reducing errors during 3D data transformation.
- A stable and efficient feature descriptor is designed, combining the structural shape attributes of the equipment 3D model with differences at various viewpoints, ensuring high recognition accuracy even with uneven 3D data density.
- The new feature descriptor enhances the descriptive ability of the 3D model, effectively reducing errors due to viewpoint changes and improving the robustness of 3D model recognition.
- While ensuring high recognition accuracy, the proposed method significantly enhances recognition speed, with an approximate recognition duration of 3.2 seconds per equipment, meeting the real-time monitoring needs of large-scale substations.

2 Related work

Over the past few years, the processing and recognition of equipment point cloud data have seen extensive use in fields such as power systems and substation equipment automation inspection. With the continuous development of laser scanning, deep learning, and computer vision technologies, improving the precision, reliability, and performance of point cloud data handling has become a hot research topic. This section reviews and analyses recent studies on point cloud feature extraction, local coordinate system establishment, and template matching, discussing the advantages and disadvantages of existing methods.

2.1 Point cloud feature extraction and descriptor construction

Feature extraction using point cloud information is a core step for achieving automatic equipment recognition. Over the years, scientists have introduced multiple feature extraction methods to enhance the precision and robustness of point cloud recognition. Ye et al. (2022) presented a point cloud-based feature extraction method based on local shape descriptors. This approach combines the point cloud data's normal direction, curvature, and local geometric features to effectively distinguish between different shapes of equipment.

By calculating local curvature changes and normal vector changes, unique geometric features of the equipment are extracted. However, while this method performs well with standard point clouds, it is sensitive to noise, particularly when the point cloud is sparse or occluded, resulting in significant accuracy degradation. To address the noise impact, Li et al. (2023a) proposed a multi-scale voxel grid-based feature extraction method. This

technique segments the point cloud into multi-scale grids and constructs feature descriptors based on the geometric information within each voxel. Empirical findings show that this approach efficiently reduces the impact of noise and enhances the robustness of point cloud features, but it remains computationally complex, especially when processing high-density point clouds, requiring greater computational resources.

In recent years, deep learning methods have seen extensive application to point cloud feature extraction, with convolutional neural networks (CNNs) being particularly useful. Sun et al. (2018) proposed a 3D convolutional neural network (3D-CNN)-based feature extraction method for point clouds. This method models point cloud data using deep learning to automatically extract both local and global features, achieving higher recognition accuracy. However, the method requires significant computational resources, especially when dealing with large point cloud datasets, leading to bottlenecks in processing speed and storage requirements.

2.2 Establishment of local coordinate system and equipment alignment

Establishing a local coordinate system for equipment point clouds is fundamental to point cloud recognition. Traditional methods often use principal component analysis (PCA) for coordinate system derivation, but PCA is sensitive to noise and occlusion, leading to poor robustness. Over the past few years, numerous approaches have been introduced to overcome this limitation. Wu et al. (2021) suggested an approach relying on the balance and spatial density of the point cloud data to establish the local coordinate system of equipment. This technique first analyses the symmetry of the point cloud data and combines the spatial distribution density of the point cloud data in various directions to deduce the directions of the coordinate axes.

This approach can effectively handle variations in equipment shape and noise interference, establishing a more robust local coordinate system. However, when dealing with highly complex equipment geometries, misjudgements may still occur, especially for devices with irregular or complicated shapes. Hu et al. (2023) proposed a deep learning-based point cloud alignment method. By training a self-supervised learning model, this method can automatically align equipment point clouds from different viewpoints, significantly improving the alignment accuracy. While this method eliminates the need for manual calibration data, it requires significant training time and computational complexity when dealing with large-scale data. To enhance robustness, Patil et al. (2017) proposed a method based on adaptive coordinate systems for point cloud alignment. This method adjusts the coordinate system's direction adaptively by detecting local features and global information of equipment point clouds, ensuring consistent coordinates for equipment regardless of its posture. While this approach handles noise and occlusion effectively, it incurs high computational costs and demands more advanced hardware.

2.3 Template matching and recognition

Early template matching methods mainly used Euclidean distance as the similarity metric. Zheng et al. (2023) employed Euclidean distance as the standard for point cloud template matching, calculating the matching error between the feature representations of the equipment for recognition and the templates in the template library. This method is simple and effective, with relatively low computational complexity, but its performance

is poor when dealing with significant shape changes, especially when equipment is partially occluded or undergoes large morphological variations.

Over the past few years, deep learning techniques have found extensive application in point cloud matching, particularly with the introduction of CNNs and GCNs, which have significantly improved the accuracy and robustness of template matching. Liu et al. (2019) proposed a point cloud template matching method based on deep convolutional neural networks. By leveraging machine learning models to automatically derive complex, high-dimensional characteristics from point clouds, this method significantly improves matching accuracy. It can adapt to changes in equipment shape and missing point clouds, but the training phase demands substantial annotated data, and the time required for training is quite extensive.

To address the issue of equipment point cloud variations, Zhang et al. (2021) introduced a point cloud approach relying on generative adversarial networks (GANs). This method generates diverse point cloud data samples to enhance the diversity of the template library, improving the robustness of template matching. Experimental results show that the GAN model effectively handles shape variations in equipment, but the training of the generated model is challenging and requires considerable computational resources.

In comparison to these methods, the approach presented in this paper combines feature descriptors with template matching, reducing computational complexity while enhancing the precision and robustness of equipment recognition.

2.4 Equipment recognition using multi-modal data fusion

Recently, the integration of point cloud and image information has gained increasing attention in equipment recognition. By combining different types of data, recognition accuracy can be enhanced, especially in complex environments. The fusion of point cloud and image data can efficiently compensate for the limitations of individual data sources. Cui et al. (2020) proposed an equipment recognition method based on integrating point cloud and image data. They utilised a deep learning model for joint training of point cloud and image information, achieving higher accuracy in equipment recognition through multi-modal feature fusion. Experimental results show that integrating point cloud information can significantly improve recognition precision, particularly when the equipment is occluded or has irregular shapes, as image data can fill in the missing point cloud information.

However, this method requires large amounts of training data and has high computational complexity. Yuan et al. (2022) proposed an equipment recognition approach utilising the integration of point cloud and LiDAR data. By combining the high-precision spatial information from LiDAR sensors with the detailed features of point cloud data, and using machine learning techniques for joint training, this method significantly improves recognition accuracy and robustness. This method is especially effective in complex environments, such as when equipment is partially occluded or when point cloud data is sparse, providing strong robustness.

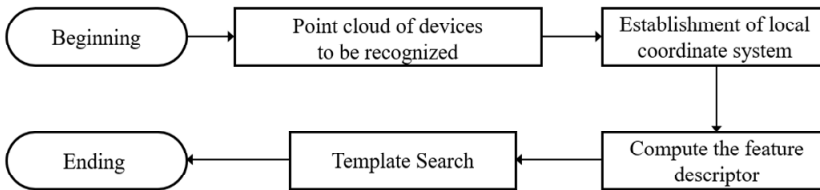
3 Method

This section introduces the proposed substation equipment point cloud recognition method. In Section 3.1, an overview of the overall design process for equipment recognition methods is provided. Then, the specific processes of the design are described in detail in Sections 3.2, 3.3, 3.4 and 3.5.

3.1 Design process

The identification algorithm process of the point cloud of substation equipment is shown in Figure 1.

Figure 1 Flowchart of point cloud recognition of substation equipment



Firstly, establish the local coordinate system of the device's point cloud for identification. This local coordinate system has translational and rotational invariance and is robust to noise. This is a crucial step in ensuring that the device point cloud is accurately identified.

Secondly, the feature descriptors of point clouds for computing devices. According to the established local coordinate system of the point cloud of the device, the point cloud is projected to the xoy, xoz and yoz planes, and each projection is finally converted into a feature vector. The three plane projected eigenvectors are connected to obtain the feature representation of the device's point cloud object.

Ultimately, the template retrieval was performed. After obtaining the feature representation of the device's point cloud object to be identified, match the feature descriptor with the feature descriptor in the template library, find the template with the smallest distance error, and complete the identification of the device.

3.2 Establish the local device point cloud's coordinate system

The commonly used method of establishing point cloud local coordinate system is mainly component analysis method (PCA), but PCA is very prone to noise and occlusions. Therefore, in this paper, the symmetry and distribution density of device point cloud in space, as shown in Figure 2. Since the substation scene is in an outdoor open environment, the terrain is flat, and the substation equipment and the ground are vertical, the z-axis orientation of the local reference system of the equipment point cloud. And the point cloud is subsequently mapped to the x-y plane to calculate the minimum enclosure box of the projection, which is the rectangle with the smallest area in all enclosure boxes, as shown in Figure 3. After obtaining the minimum surround frame of the device point cloud, take the boundary of the surrounding frame as the x-axis and the longer edge as the y-axis. Then establish the minimum surround box of the device point cloud as the

bottom side, and take the centre of the minimum surround box as the origin of the local coordinate system of the device point cloud, as illustrated in Figure 4.

Figure 2 Flowchart of establishing a local coordinate system of equipment point cloud

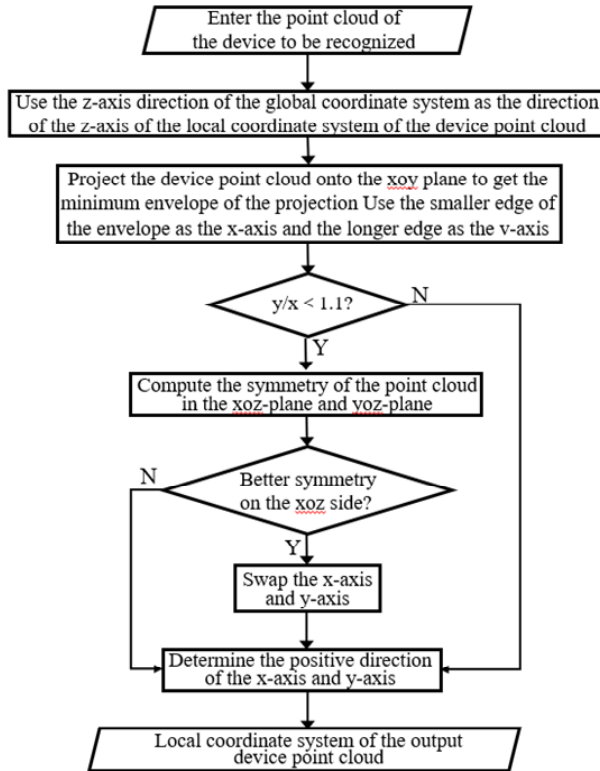
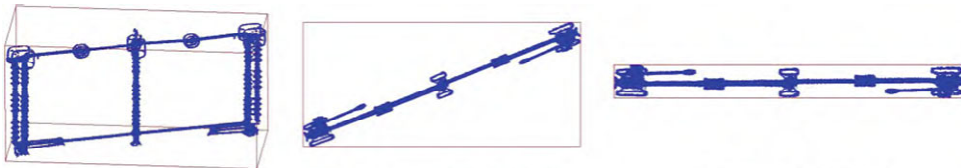


Figure 3 Minimum bounding box of the projection of equipment point cloud in xoy plane (see online version for colours)



When the proportion between the two edges of the minimum enclosure is less than 1.1, the horizontal and vertical axes are judged for the first time; however, due to the possibility of noise interference, further judgement is needed to identify the horizontal and vertical axes. This requires analysing the symmetry of the device point cloud about the yoz and xoz planes on the basis of the x and y axes determined in the first time.

As illustrated in Figure 5, if the device point cloud object has better symmetry about the xoz plane, then the horizontal and vertical axes are modified; otherwise, the current x-axis and y-axis are unchanged.

Figure 4 Determination of x and y axes of the local coordinate system (see online version for colours)

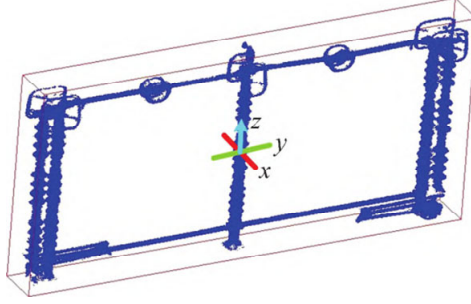
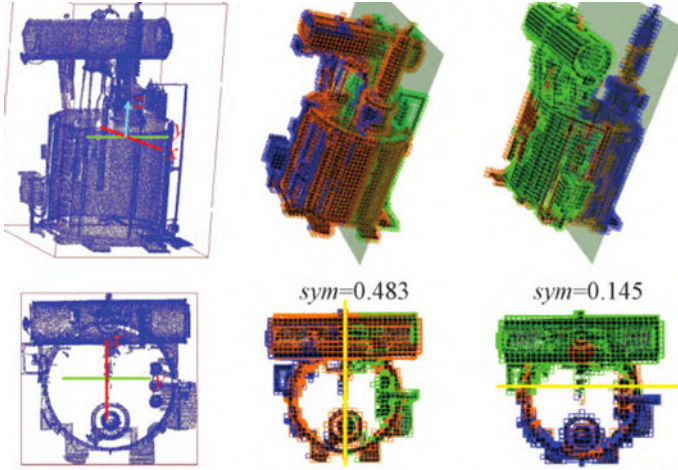


Figure 5 The symmetry of equipment point cloud on plane xoz and plane yoz (see online version for colours)



To calculate the symmetry of a device point cloud about the plane pl , initially, the smallest bounding box for the device's point cloud is subjected to voxel partitioning, resulting in the voxel grid of the point cloud, denoted as V . The determination of voxel size necessitates consideration of the data density of the point cloud, the impact of noise, and computational efficiency. Through experimentation, the voxel size is defined as 0.1 meters.

If $V(i, j, k)$ contains a point within the object's point cloud, then $V(i, j, k) = 1$; otherwise, $V(i, j, k) = 0$. The plane pl splits the voxel grid into two sections, denoted as pl^+ and pl^- , where the number of voxels with $V(i, j, k) = 1$ in each of these sections is denoted as n_{pl^+} and n_{pl^-} , respectively. When the two symmetrical parts have $V(i, j, k) = 1$, the voxel is considered to possess symmetry. The number of all symmetrical voxels in V is denoted as n_{sym} . The symmetry of the object point cloud with respect to the plane pl is calculated according to equation (1).

$$sym(pl) = \frac{n_{sym}}{2 \cdot \min(n_{pl^+}, n_{pl^-})} \quad (1)$$

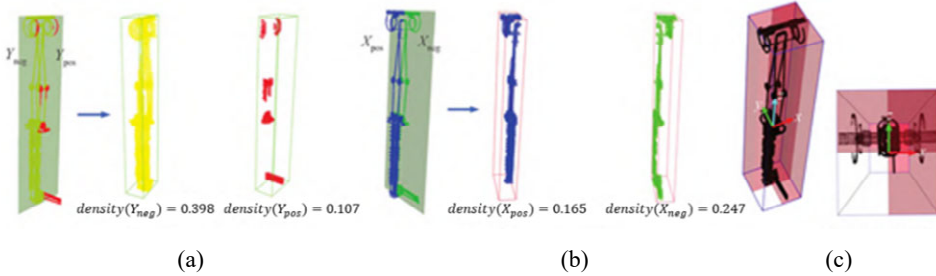
After determining the x and y axes, the distribution density of the cloud of points in space serves to identify the positive directions of the x and y axes. The cloud of points is split into two parts by the xoz plane and the yoz plane, as shown in Figures 6(a) and 6(b). The two sections separated by the xoz plane are labelled as Y_{pos} and Y_{neg} , respectively, while the two sections separated by the yoz plane are labelled as X_{pos} and X_{neg} . According to equation (2), the volume densities of these four parts are calculated as follows:

$$density(P^*) = \frac{n_{P^*}}{n_{scale}} \quad (2)$$

where n_{P^*} indicates the voxel count in part P^* , where $V(i, j, k) = 1$; n_{scale} represents the overall count of voxels in part P^* , including voxels, where $V(i, j, k) = 1$ and $V(i, j, k) = 0$.

Based on the calculated volume densities of these four parts, the direction of the part with the larger volume density is taken as the forward direction of the respective coordinate axis. For example, for the two parts X_{pos} and X_{neg} divided by the yoz plane, if the volume density of X_{pos} is greater than that of X_{neg} , then the forward direction of the x -axis coordinates moves towards X_{pos} . Similarly, the forward direction of the y -axis can be determined based on the volume densities of Y_{pos} and Y_{neg} . Using this approach, the point's local coordinate system for the device is established, as illustrated in Figure 6(c). This local coordinate system is invariant under translation and rotation, guaranteeing resistance to noise.

Figure 6 Determination of the positive direction of x and y axes, (a) divided by the xoz plane (b) divided by the yoz plane (c) establishment of the local reference coordinate system (see online version for colours)



3.3 Feature description

This paper defines a novel feature descriptor by combining the variations in the form of the substation equipment point cloud with the equipment image. The specific calculation steps are outlined as follows:

- Step 1 Segment the smallest bounding box for the equipment point cloud and divide it into a $12 \times 12 \times 12$ voxel grid, where the voxel size is

$$\begin{cases} l = \frac{L}{12}; \\ w = \frac{W}{12}; \\ h = \frac{H}{12}. \end{cases} \quad (3)$$

where L , W and H represent the dimensions (length, width, and height) of the minimum enclosure box for the equipment point cloud, respectively; l , w and h denote the dimensions of each voxel.

A voxel space V is established for the equipment point cloud object, through which a 3D spatial distribution matrix $M_{12 \times 12 \times 12}$ is obtained for the equipment point cloud object. $M_{12 \times 12 \times 12}$ represents the spatial arrangement features of the object point cloud within three-dimensional space. If a point falls into a voxel $V(i, j, k)$, the corresponding value of the distribution matrix is set to 1, i.e., $M(i, j, k) = 1$; otherwise, $M(i, j, k) = 0$.

Step 2 The equipment point cloud is mapped to the xoy, xoz, and yoz planes, resulting in three two-dimensional distribution matrices: $M_{12 \times 12}^{xoy}$, $M_{12 \times 12}^{xoz}$ and $M_{12 \times 12}^{yoz}$.

$$M^{xoy}(i, j) = \begin{cases} 1, & \sum_{k=1}^{12} M(i, j, k) \neq 0; \\ 0, & \text{otherwise} \end{cases} \quad (4)$$

$$M^{xoz}(i, j) = \begin{cases} 1, & \sum_{k=1}^{12} M(i, k, j) \neq 0; \\ 0, & \text{otherwise} \end{cases} \quad (5)$$

$$M^{yoz}(i, j) = \begin{cases} 1, & \sum_{k=1}^{12} M(k, i, j) \neq 0; \\ 0, & \text{otherwise} \end{cases} \quad (6)$$

Step 3 Convert the two-dimensional distribution matrix of each projection plane into a feature representation, and concatenate the three feature representations to construct the final feature descriptor of the equipment point cloud object. For a given projection plane's two-dimensional distribution matrix $M_{12 \times 12}^*$, it is transformed into a feature representation v_{24}^* according to equation (7):

$$v_{24}^*(i) = \begin{cases} \sum_{j=1}^{12} M^*(i, j), & i \leq 12; \\ \sum_{j=1}^{12} M^*(j, i), & \text{otherwise} \end{cases} \quad (7)$$

Each projection plane is converted into a 24-dimensional feature vector. Then, the feature vectors of the three projection planes are concatenated to obtain the final feature descriptor $f(v_{24}^{xoy}, v_{24}^{xoz}, v_{24}^{yoz})$, with a dimensionality of $24 \times 3 = 72$.

3.4 Template matching

Since there is currently no publicly available dataset of point clouds in substation scenarios, nor a public template library for substation electrical equipment, this paper establishes a template library for electrical equipment, which includes 54 standard electrical equipment templates. The standard electrical equipment includes categories such as circuit breakers, disconnectors, and isolating switches. Each type of electrical equipment is assigned a unique identification number. The feature descriptor of each template point cloud is calculated and stored together with the corresponding template's category, identification number, and 72-dimensional feature descriptor information. The template library is organised as a 54×72 two-dimensional matrix and stored in a structured format, facilitating retrieval. When the shape of a device changes or new equipment types needs to be identified, the template library can be updated or supplemented to ensure its dynamic consistency.

During the template matching stage, after obtaining the feature representation of the target equipment point cloud, the similarity between this representation and the feature representations of each template in the template library is calculated to find the best-matching template. Since the Euclidean distance assessment approach is simpler and more effective than other methods, the Euclidean distance between the feature representation of the target equipment point cloud and the feature descriptor of the template is calculated according to equation (8) and used as the discrepancy between the two.

$$\varepsilon(f_o, f_{o'}) = \sum_{i=1}^{72} (f_o(i) - f_{o'}(i))^2 \quad (8)$$

where f_o represents the feature descriptor of a template in the template library; f_i represents the feature descriptor of the equipment point cloud to be identified.

4 Experiments and analysis

4.1 Experiment details

The computer used in the experiment is configured with an Intel® Core™ i5-10300H CPU, 8 GB of memory, and a 64-bit Windows 10 operating system. The experimental platform is Visual Studio 2019, utilising the PCL open-source C++ library for point cloud programming. The substation equipment point cloud recognition algorithm proposed in this paper was evaluated using 90 point cloud datasets of equipment for identification. The experimental data in this paper was obtained by using a 3D laser scanner mounted on a vehicle to scan parts from the Songshan 500 kV substation.

4.2 Compare with other methods

For each equipment point cloud to be identified, its feature descriptor is calculated and then compared with the feature descriptors of all templates in the template library to find the template with the highest similarity. This completes the recognition of the equipment's point cloud. Among the 90 tested equipment point clouds, 81 were correctly recognised, while 9 were misidentified, resulting in a recognition accuracy of 90%. The

average time to identify one equipment point cloud was 3.2 seconds, showing a comparatively high recognition speed.

The method introduced in this study was evaluated against two other existing point cloud of substation equipment recognition methods, and the findings are presented in Table 1. The recognition accuracy of all three methods exceeds 85%, with the proposed algorithm achieving 90%, marginally below the 92.33% performance reported in Yuan et al. (2023), but higher than the 87.78% accuracy in Guo et al. (2019). Although there is a minor variance in accuracy, the proposed algorithm has a recognition time of only 3.20 seconds, which is considerably faster than the 19.41 seconds in Arastounia and Lichti (2013) and 17.56 seconds in Ji et al. (2019).

The accuracy difference may be related to feature extraction and model complexity. The higher-accuracy method in Yuan et al. (2023) may have used more complex feature descriptors and deep learning models, while the proposed algorithm simplifies the feature extraction process, reducing computational complexity and thus significantly shortening recognition time. This makes it more suitable for applications that require fast responses.

In terms of balancing efficiency and accuracy, the proposed algorithm effectively reduces recognition time while maintaining high accuracy, making it suitable for real-time monitoring and dynamic recognition tasks for substation equipment. Although its accuracy is slightly lower than that of Yuan et al. (2023), the shorter recognition time gives it a significant advantage in practical applications that demand high real-time performance. Therefore, the proposed algorithm shows good potential for application in equipment point cloud recognition.

Table 1 Comparison of different methods

<i>Algorithm</i>	<i>Recognition time (s)</i>	<i>Recognition accuracy (%)</i>
Proposed algorithm	3.20	90.00
Method in Guo et al. (2019)	17.56	87.78
Method in Hu (2020)	19.41	92.33

As shown in Table 2, when comparing the performance of our, GOOD (a), and VFH (b) methods, it can be observed that our method outperforms other methods in terms of precision, recall, and accuracy, exhibiting strong overall advantages. Specifically, the recall rate of our method in all test samples remained above 0.659 and reached a maximum of 0.738, which was significantly higher than that of GOOD (a) and VFH (b), indicating that the method has strong recognition ability when retrieving matches, and can effectively reduce missed detections. In addition, in terms of accuracy, the highest value of this method is 0.710, indicating that it can maintain a low false detection rate while ensuring the recall rate, thus improving the overall recognition effect. In contrast, the GOOD (a) method performs relatively well in terms of recall rate, reaching a maximum of 0.719, indicating that it has a wide coverage of sample matching. However, its precision and accuracy are significantly lower than our method, with the highest being 0.622 and 0.544, respectively, indicating that although this method can retrieve more matching samples, it has more false detections and reduces the overall accuracy. On the other hand, the accuracy of the VFH (b) method is relatively high, reaching a maximum of 0.698, which is slightly better than that of GOOD (a), but the recall rate is generally low, resulting in its limited effect in some sample matching tasks. In addition, the overall accuracy of the VFH method is between GOOD (a) and our method, reaching a

maximum of 0.568, which is still significantly lower than the 0.666 of our method. Further analysis of the advantages of our method shows that it exhibits relatively stable performance in all three indicators, especially while ensuring a high recall rate, it still maintains a high precision and accuracy.

Table 2 Performance comparison with other existing methods

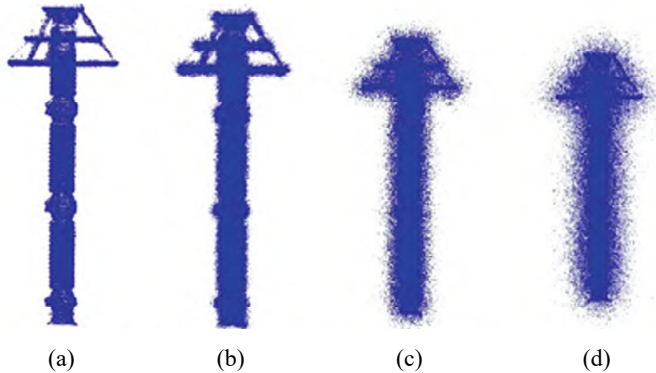
<i>Our</i>			<i>GOOD (a)</i>			<i>VFH (b)</i>		
<i>Precision</i>	<i>Recall</i>	<i>Accuracy</i>	<i>Precision</i>	<i>Recall</i>	<i>Accuracy</i>	<i>Precision</i>	<i>Recall</i>	<i>Accuracy</i>
0.696	0.721	0.640	0.503	0.615	0.410	0.575	0.629	0.472
0.651	0.659	0.552	0.516	0.581	0.400	0.698	0.615	0.552
0.687	0.706	0.619	0.589	0.719	0.544	0.631	0.668	0.544
0.710	0.738	0.666	0.622	0.613	0.497	0.649	0.649	0.544
0.702	0.727	0.650	0.607	0.671	0.527	0.653	0.677	0.568

4.3 Ablation experiments

To evaluate the resilience of the equipment point cloud recognition method presented in this study, experiments were conducted under scenarios involving noise, irregular point cloud density, and occlusions.

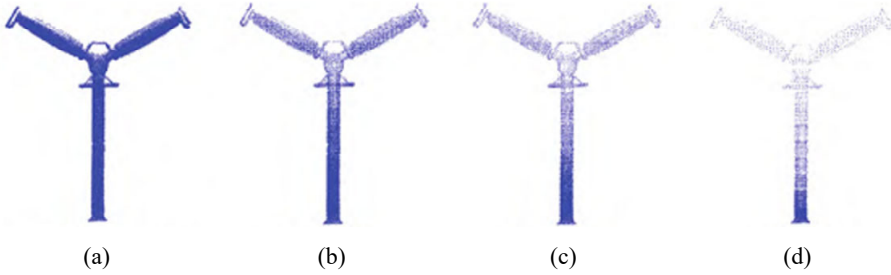
- 1 Noise: Gaussian noise with different variances σ was added to the 90 equipment point clouds to be identified, as illustrated in Figure 7.

Figure 7 Equipment point cloud with different degree of Gaussian noise, (a) original equipment point cloud (b) $\sigma = 0.05$ (c) $\sigma = 0.15$ (d) $\sigma = 0.30$ (see online version for colours)



- 2 Uneven point cloud density: the 90 equipment point cloud objects were divided into layers along the z-axis at intervals of 0.5 m, and voxel down-sampling was applied to each layer. The voxel size for the 0th layer was set as $VoxelSize_0$, and the voxel size for the i^{th} layer was set as $VoxelSize_i$. Different levels of down-sampling were applied to the equipment point clouds by setting different $VoxelSize$ values, as illustrated in Figure 8.

Figure 8 Equipment point cloud with different degree of uneven density, (a) original equipment point cloud (b) 0.005 (c) 0.010 (d) 0.030 (see online version for colours)



3 Occlusion: a variable cube with a fixed angle was applied to segment the point cloud of the equipment objects, as depicted in Figure 9. The rate of occlusion for the point cloud is determined by calculating the proportion of points that are blocked or removed relative to the total points in the original point cloud.

Figure 9 Equipment point cloud with different degrees of occlusion, (a) no occlusion (b) 15% occlusion (c) 25% occlusion (d) 60% occlusion (see online version for colours)

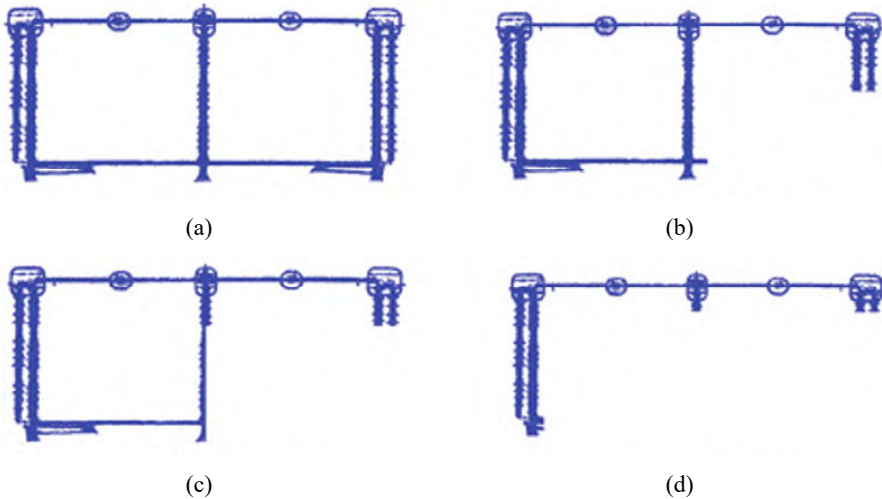
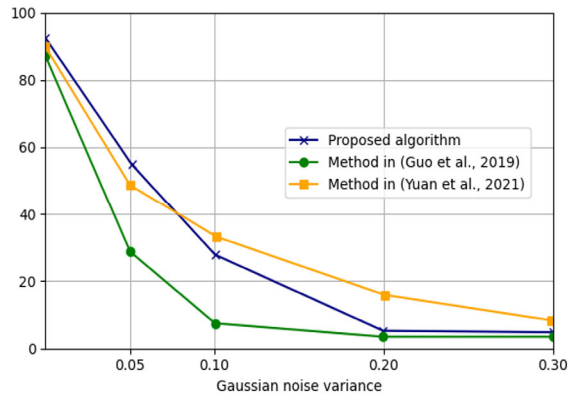
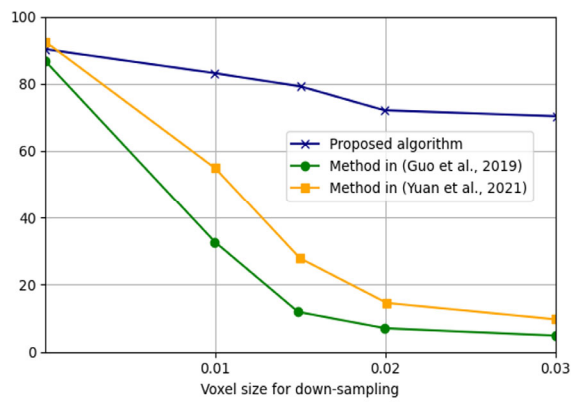


Figure 10 shows the comparative results of the suggested algorithm and two other substation equipment point cloud recognition algorithms under conditions of noise, uneven density, and occlusion. From Figure 10(a), it is observed that as the noise level in the point cloud increases, the recognition precision of all three methods drops rapidly. On noise-free data, all three methods achieve good recognition performance, but under high noise levels, the proposed method achieves slightly superior to the other two methods. This is because the method in Guo et al. (2019) uses the cosine value of the angle between the centroid of the subspace and the centroid of the entire point cloud as the subspace feature.

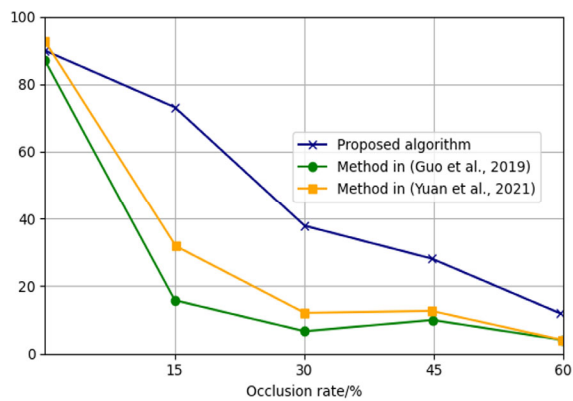
Figure 10 Comparison of recognition accuracy of different algorithms, (a) under noise conditions (b) when the point cloud density is uneven (c) under occlusion conditions (see online version for colours)



(a)



(b)



(c)

When the point cloud is noisy, the characteristics of the subspaces containing noise points deviate from 0. If the point cloud contains too numerous noise points, which results in significant changes to the subspace feature vectors, making it difficult to effectively recognise the point cloud. The method in (Yuan et al., 2023) predicts the template by identifying the planar characteristics of the equipment point cloud. However, since substation equipment is generally symmetrical along the central axis, the extraction of planar features requires high precision. When the point cloud contains a large amount of noise, the planar features of the equipment point cloud may fail to select the correct template, leading to recognition errors. In contrast, the descriptor introduced in this study leverages the existence of points in the 2D grid of each projection plane, which helps mitigate the negative impact of noise on recognition.

From Figure 10(b), it can be seen that the proposed equipment point cloud recognition algorithm maintains an identification accuracy of over 70% even when the point cloud density is uneven, showing significant advantages over the other two recognition methods. The method in Guo et al. (2019) uses the cosine value of the angle between the centroid of the subspace and the centroid of the entire point cloud as the subspace feature. This method is highly sensitive to point cloud density. When the point cloud density is uneven, the overall centroid of the point cloud undergoes severe shifts, resulting in features that cannot effectively recognise the equipment point cloud. Consequently, as the sampling level increases, the recognition accuracy drops rapidly. The method in Yuan et al. (2023) uses the RANSAC algorithm to extract planar features. However, when the point cloud density is uneven, planar features cannot be accurately extracted, leading to a decline in recognition accuracy. In contrast, the proposed equipment point cloud recognition method describes the equipment point cloud based on the existence of points in the 2D grid of each projection plane. When the point cloud density is uneven, the shape features of the equipment point cloud are not directly affected. Therefore, the proposed feature descriptor can still effectively describe the equipment point cloud, maintaining a high recognition accuracy.

From Figure 10(c), it can be seen that once the occlusion rate exceeds 30%, the recognition accuracy of all three methods decreases. This is due to the presence of some substation equipment with central axis symmetry. When occlusion is present in the point cloud, the plane normal vectors extracted by the RANSAC algorithm in the method of Yuan et al. (2023) become inaccurate, leading to a decline in recognition accuracy. The method in Yuan et al. (2023) is more affected by occlusion because when occlusion occurs in the point cloud, not only does the centroid of the entire point cloud shift, but the subspace features of the missing parts also become 0, which causes the final feature descriptor to fail to describe the original equipment point cloud, resulting in lower recognition accuracy. In contrast, the proposed method extracts the feature descriptor of the equipment point cloud based on its shape, which provides strong descriptive ability. However, when occlusion is present, the shape of the point cloud changes to some extent, leading to a decrease in recognition accuracy. Nonetheless, it still outperforms the other two methods overall.

In order to solve the significant performance degradation under high occlusion rate (more than 30%), we will explore the improved feature extraction algorithm, which can develop an algorithm that can adjust the strategy adaptively according to the occlusion situation. When high occlusion rate is detected, it automatically shifts to focus on local feature extraction. An in-depth analysis of the unblocked local point cloud area extracts representative local features to make up for the lack of overall shape features. Multi-scale

feature fusion can also be used, which shows different performance of point cloud features at different scales. When high occlusion rate is combined with large-scale features to grasp the general information of the overall structure, small-scale features can be used to capture the details of the unblocked part, and the two can be effectively fused to enhance the expression ability of feature descriptors to the occluded point cloud. In terms of optimising the data processing flow, the occluded point cloud data can be enhanced and repaired before identification.

With the help of a generative adversarial network (GAN)-based method, the occluded part of the data can be generated according to the characteristics of the unoccluded part of the point cloud, and the noise or error data can be repaired at the same time. Improve data quality; a model can also be established to predict the shape and location of the occluded area. According to the prior knowledge of the unoccluded part of the point cloud and equipment, the predicted occluded area can be compensated and adjusted during the identification process to reduce the impact of occlusion. In addition, other techniques for processing closed data are also feasible paths. In multi-modal data fusion technology, visual image data can be combined, and its rich texture and colour information can be complementary to the geometric information of point cloud data under high occlusion rate. The deep learning algorithm is used to fuse the two to participate in the device point cloud recognition and improve the accuracy.

On the other hand, if the point cloud data is obtained by using lidar, its multiple echo information can be used. When occluding, subsequent echoes may penetrate or reflect from the edge of the occlusion to obtain partial information of the occluded object, so as to gain a more comprehensive understanding of the point cloud scene and enhance the recognition ability of the occluded device. In the semantic segmentation technology based on deep learning, a dedicated model can be trained for the point cloud data of substation equipment under high occlusion rate, and the model can learn the characteristic patterns of equipment under various occlusion situations through a large number of labeled samples. According to the context, the occluded part can be inferred to achieve accurate segmentation and recognition. It can also use pre-trained models on large-scale general point cloud datasets for transfer learning, and fine-tune the characteristics of high occlusion rate to quickly utilise existing model knowledge, reduce the amount of training data and time, and better adapt to high occlusion rate closed data scenarios to improve recognition performance.

5 Conclusions

This paper proposes a novel approach to address the issue of substation equipment point cloud recognition. First, the local reference system for the target equipment point cloud is established by utilising the balance and spatial distribution of the point cloud of the equipment in space. Second, a feature descriptor is defined based on the differences in the geometric structure of the point cloud of the equipment and the equipment view. This descriptor is used for the description and recognition of point clouds. A template library containing 54 template point clouds is created, and the feature descriptors of the target equipment point cloud are matched with those in the template library to find the template with the smallest matching error, thereby completely identifying the equipment point cloud. Finally, experiments validate the effectiveness and advantages of the suggested

approach. The recognition accuracy reaches 90%, and the average time to recognise a single piece of equipment is 3.2 seconds, effectively balancing recognition accuracy and efficiency. When the target point cloud's density is uneven, the proposed method can still sustain a recognition accuracy of over 70%. Moreover, the established local coordinate system of the equipment point cloud can be used to calculate the transformation matrix linking the target point cloud and the template point cloud, facilitating subsequent 3D reconstruction of substation scenarios.

Declarations

This work was supported by State Grid Shanxi Electric Power Company Technology Project: Research and application of precise diagnosis technology for infrared three-dimensional imaging and thermal anomalies (No. 52053023000Y).

The author declares that it does not have any known interests or personal relationships that could potentially influence the reported work in this paper.

References

- Al-Durgham, K. (2014) *Geometric Features Extraction and Automated Registration of Static Laser Scans Using Linear Features*, Doctoral dissertation, MSc thesis, University of Calgary, Calgary, Canada.
- Arastounia, M. and Lichti, D.D. (2013) 'Automatic extraction of insulators from 3D LiDAR data of an electrical substation', *ISPRS Annals of the Photogrammetry, Remote Sensing and Spatial Information Sciences*, pp.19–24.
- Arastounia, M. and Lichti, D.D. (2014) 'Segmentation of planar surfaces in LiDAR point clouds of an electrical substation by exploring the structure of points neighbourhood', *ISPRS – International Archives of the Photogrammetry, Remote Sensing and Spatial Information Sciences*, pp.55–62.
- Arastounia, M. and Lichti, D.D. (2015) 'Automatic object extraction from electrical substation point clouds', *Remote. Sens.*, Vol. 7, No. 11, pp.15605–15629.
- Azevedo, D.M., Marotti, A., Cardoso, A., Lamounier, E.A., Lima, G., Araujo, A.L., Guttler, C., Rocha, R.D. and Bartholomeu, C. (2021) 'Development of BIM (building information modeling) concept applied to projects of substations integrated with the geographic intelligence system (GIS)', *WSEAS Transactions on Power Systems*, Vol. 16, pp.1–7.
- Cui, Y., Chen, R., Chu, W., Chen, L., Tian, D., Li, Y. and Cao, D. (2020) 'Deep learning for image and point cloud fusion in autonomous driving: a review', *IEEE Transactions on Intelligent Transportation Systems*, Vol. 23, No. 2, pp.722–739.
- Guo, W., Ji, Y., Luo, Y. and Zhou, Y. (2019) 'Substation equipment 3D identification based on KNN classification of subspace feature vector', *Journal of Intelligent Systems*, Vol. 28, pp.807–819.
- Hu, L. (2020) 'Application of AutoCAD's 3D modeling function in industrial modeling design', *Computer-Aided Design and Applications*, Vol. 18, No. 1.
- Hu, P., Ho, E.S. and Munteanu, A. (2023) 'AlignBodyNet: deep learning-based alignment of non-overlapping partial body point clouds from a single depth camera', *IEEE Transactions on Instrumentation and Measurement*, Vol. 72, pp.1–9, <https://doi.org/10.1109/TIM.2022.3222501>.

- Jawad, M., Nadeem, M.S., Shim, S., Khan, I.R., Shaheen, A., Habib, N., Hussain, L. and Aziz, W. (2020) 'Machine learning based cost effective electricity load forecasting model using correlated meteorological parameters', *IEEE Access*, Vol. 8, pp.146847–146864, <https://doi.org/10.1109/ACCESS.2020.3014086>.
- Ji, Y., Liu, D.D., Luo, Y. et al. (2019) 'Recognition of three-dimensional substation equipment based on Hough transform', *Journal of Zhengzhou University (Engineering Science)*, Vol. 40, No. 3, pp.1–6, 12.
- Karantzalos, K. and Paragios, N. (2010) 'Large-scale building reconstruction through information fusion and 3-D priors', *IEEE Transactions on Geoscience and Remote Sensing*, Vol. 48, pp.2283–2296.
- Kokorus, M., Eyrich, W.K. and Zacharias, R. (2016) 'Innovative approach to the substation design using building information modeling (BIM) technology', *2016 IEEE/PES Transmission and Distribution Conference and Exposition (T&D)*, pp.1–5.
- Li, H., Guan, H., Ma, L., Lei, X., Yu, Y., Wang, H., Delavar, M.R. and Li, J. (2023a) 'MVPNet: a multi-scale voxel-point adaptive fusion network for point cloud semantic segmentation in urban scenes', *Int. J. Appl. Earth Obs. Geoinformation*, Vol. 122, p.103391, <https://doi.org/10.1016/j.jag.2023.103391>.
- Li, R., Gan, L., Liu, Y., Di, Y. and Wang, C. (2023b) 'A model-driven approach for fast modeling of three-dimensional laser point cloud in large substation', *Scientific Reports*, Vol. 13, No. 1, p.16092.
- Liu, Y., Fan, B., Xiang, S. and Pan, C. (2019) 'Relation-shape convolutional neural network for point cloud analysis', *2019 IEEE/CVF Conference on Computer Vision and Pattern Recognition (CVPR)*, pp.8887–8896.
- Nader, A., Abdelhamid, H. and Ridha, M. (2021) 'A quantum-behaved particle-swarm-optimization-based KNN classifier for improving WSN lifetime', *Sensor Data Analysis and Management*, <https://doi.org/10.1002/9781119682806.ch7>.
- Patil, A.K., Holi, P., Lee, S.K. and Chai, Y.H. (2017) 'An adaptive approach for the reconstruction and modeling of as-built 3D pipelines from point clouds', *Automation in Construction*, Vol. 75, pp.65–78.
- Sun, T., Li, M., Wang, W. and Liu, C. (2021) '3D reconstruction of UAV remote sensing sequence image based on iterative constraint weighting', *International Journal of Information and Communication Technology*, Vol. 19, No. 4, pp.371–390.
- Sun, T., Liu, J., Kan, J. and Sui, T. (2022) 'Research on target classification method for dense matching point cloud based on improved random forest algorithm', *International Journal of Information and Communication Technology*, Vol. 21, No. 3, pp.290–303.
- Sun, T., Liu, M., Ye, H. and Yeung, D.Y. (2018) 'Point-cloud-based place recognition using CNN feature extraction', *IEEE Sensors Journal*, Vol. 19, pp.12175–12186, <https://doi.org/10.1109/JSEN.2019.2937740>.
- Wu, Q., Yang, H., Wei, M., Remil, O., Wang, B. and Wang, J. (2018) 'Automatic 3D reconstruction of electrical substation scene from LiDAR point cloud', *ISPRS Journal of Photogrammetry and Remote Sensing*, <https://doi.org/10.1016/j.isprsjprs.2018.04.024>.
- Wu, Y., Shang, J. and Xue, F. (2021) 'RegARD: symmetry-based coarse registration of smartphone's colorful point clouds with CAD drawings for low-cost digital twin buildings', *Remote. Sens.*, Vol. 13, p.1882, <https://doi.org/10.3390/rs13101882>.
- Yang, Y., Sun, Y., Zhang, F. and Liu, M. (2024) 'An integrated approach for accurate 3D point cloud recognition of substation equipment using PSO and kNN classification', *Journal of Combinatorial Mathematics and Combinatorial Computing*, <https://doi.org/10.61091/jcmcc119-20>.
- Ye, J., Zhang, X. and Xu, B. (2023) 'Construction quality inspection method of substation fabricated structure based on 3D laser scanning', *Journal of Physics: Conference Series*, Vol. 2479.

- Ye, T., Yan, X., Wang, S., Li, Y. and Zhou, F. (2022) ‘An efficient 3-D Point cloud place recognition approach based on feature point extraction and transformer’, *IEEE Transactions on Instrumentation and Measurement*, Vol. 71, pp.1–9, <https://doi.org/10.1109/TIM.2022.3209727>.
- Yu, X., Tang, L., Rao, Y., Huang, T., Zhou, J. and Lu, J. (2021) ‘Point-BERT: pre-training 3D point cloud transformers with masked point modeling’, *2021 IEEE/CVF Conference on Computer Vision and Pattern Recognition (CVPR)*, pp.19291–19300.
- Yuan, Q., Chang, J., Luo, Y., Ma, T. and Wang, D. (2023) ‘Automatic cables segmentation from a substation device based on 3D point cloud’, *Machine Vision and Applications*, Vol. 34, No. 1, p.9.
- Yuan, Q., Luo, Y. and Wang, H. (2022) ‘3D point cloud recognition of substation equipment based on plane detection’, *Results in Engineering*, <https://doi.org/10.1016/j.rineng.2022.100545>.
- Zhang, H., Wang, C., Tian, S., Lu, B., Zhang, L., Ning, X. and Bai, X. (2023) ‘Deep learning-based 3D point cloud classification: a systematic survey and outlook’, *Displays*, Vol. 79, p.102456, <https://doi.org/10.1016/j.displa.2023.102456>.
- Zhang, J., Chen, X., Cai, Z., Pan, L., Zhao, H., Yi, S., Yeo, C., Dai, B. and Loy, C.C. (2021) ‘Unsupervised 3D shape completion through GAN inversion’, *2021 IEEE/CVF Conference on Computer Vision and Pattern Recognition (CVPR)*, pp.1768–1777.
- Zhang, Z., Shi, W., Wen, D., Wu, Y., Zhou, J. and Bian, K. (2024) ‘Research on point cloud segmentation method based on local and global feature extraction of electricity equipment’, *IEEE Access*, Vol. 12, pp.143402–143412, <https://doi.org/10.1109/ACCESS.2024.3468012>.
- Zhang, Z.Q., Yang, H.B., Chen, Y. et al. (2018) ‘Rapid modeling method for substations based on component matching’, *Computer Applications and Software*, Vol. 35, No. 7, pp.69–75, 210.
- Zheng, L., Hu, Z., Yao, M., Xu, P. and Ma, J. (2023) ‘Point cloud based hand gesture recognition using template matching’, *J. Intell. Fuzzy Syst.*, Vol. 46, pp.2615–2627, <https://doi.org/10.3233/jifs-233120>.
- Zhu, H., Zhang, Z., Zhao, J., Duan, H., Ding, Y., Xiao, X. and Yuan, J. (2024) ‘Scene reconstruction techniques for autonomous driving: a review of 3D Gaussian splatting’, *Artif. Intell. Rev.*, Vol. 58, p.30, <https://doi.org/10.1007/s10462-024-10955-4>.